Extragalactic jets from every angle
Proceedings IAU Symposium No. 313, 2014
F. Massaro, C. C. Cheung, E. Lopez, A. Siemiginowska, eds.

doi:10.1017/S1743921315001829

The jet of the quasar 4C+21.35 from parsec to kiloparces scales and its role in high energy photon production

Svetlana G. Jorstad[1,2], Alan P. Marscher[1], Daria A. Morozova[2], Vishal Bala[1], Ivan Agudo[3,1,4], José L. Gómez[4], Anne Lähteenmäki[5,6], Valeri M. Larionov[2], Paul S. Smith[7] and Merja Tornikoski[5]

[1]IAR, Boston University, 725 Commonwealth Avenue, Boston, MA 02215, USA

[2]Astronomical Institute, St. Petersburg State University, Universitetskij Pr. 28, Petrodvorets, 198504 St. Petersburg, Russia

[3]JIVE, Postbus 2, NL-7990 AA Dwingeloo, The Netherlands

[4]Instituto de Astrofísica de Andalucía, CSIC, Apartado 3004, 18080, Granada, Spain

[5]Aalto University Metsähovi Radio Observatory Metsähovintie 114, FIN-02540 Kylmälä, Finland

[6]Aalto University Department of Radio Science and Engineering, P.O. BOX 13000, FI-00076 AALTO, Finland

[7]Steward Observatory, University of Arizona, Tucson, AZ 85721-0065, USA

Abstract. We present an analysis of the parsec-scale jet structure of the quasar 4C+21.35 with a resolution of 0.1 milliarcseconds based on 63 epochs of Very Long Baseline Array observations at 43 GHz from 2007 June to 2014 May along with the *Fermi* LAT γ-ray light curve and multi-frequency optical photometric and polarimetric data. We find that the innermost jet of the quasar consists of a very compact core of size $\sim$0.03 mas, as well as feature $A1$ located 0.16$\pm$0.03 mas from the core. The distance of $A1$ remains fairly stable, but its position angle with respect to the core changes from -10 to $+10$ deg. We detect 4 superluminal knots in the inner jet with apparent speeds ranging from $10c$ to $20c$. The first two components appeared in the jet during the high γ-ray state of the quasar from mid-2010 to early 2011, while the fourth knot appears to be connected with the γ-ray active state in late 2013 - early 2014. The first knot can be associated with the dramatic VHE flare in 2010 June and possesses an extreme Doppler factor $\sim$60. We find that maxima in the γ-ray light curve coincide with epochs of interaction between the moving knots and the core and feature A1. This suggests that the core and $A1$ are recollimation shocks where γ-ray flares occur. The *Chandra* 0.5-6 keV image reveals the existence of X-ray emission in the kiloparsec scale jet of the quasar that can be explained via inverse Compton scattering off the cosmic microwave background by relativistic electrons if no deceleration occurs between the parsec- and kiloparsec-scale jets.

Keywords. quasars: individual (4C+21.35, 1222+216), relativistic processes, gamma rays: observations, polarization

1. Introduction

The quasar 4C+21.35 (1222+216; z=0.435) is one of the most intriguing of the extreme active galactic nuclei (AGN) known as "blazars." The central black hole (BH) has a mass of $6\times10^8 M_\odot$ (Farina *et al.* 2012). The BH is surrounded by an accretion disk with a luminosity of 5×10^{46} erg s^{-1}, and broad line region (BLR) of radius 0.23 pc (Tavecchio *et al.* 2011). A dusty torus of T$\sim$1200 K is located 1-2 pc from the BH (Malmrose *et al.*

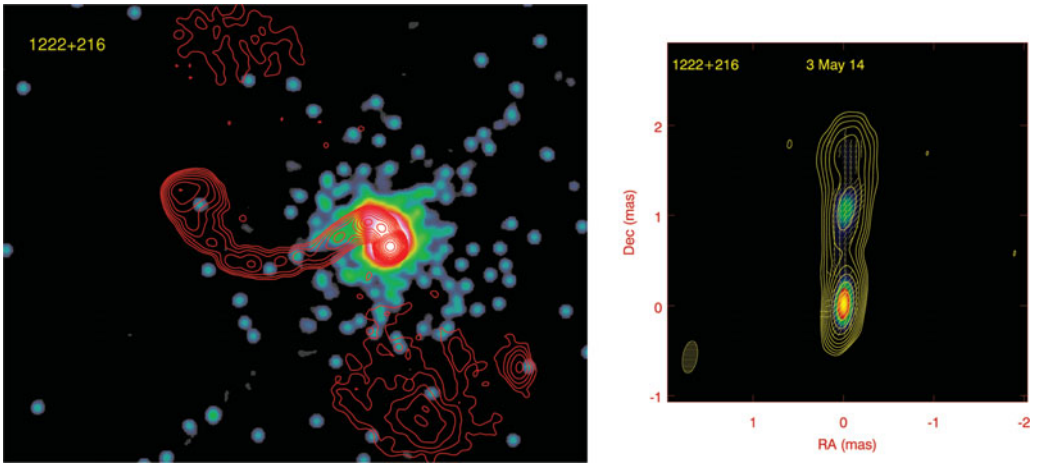

Figure 1. *Left:* Chandra (color scale) and VLA 5 GHz (contours) images of 4C+21.35; contours are in factors of 2 of the peak intensity of 0.93 Jy/beam. The images are convolved with a beam of FWHM 0.5×0.5 arcsec^2. *Right:* VLBA image of the inner jet at 43 GHz; contours are in factors of 2 of the peak intensity of 0.99 Jy/beam; color scale corresponds to polarized intensity with peak = 62.5 mJy/beam; line segments within the contours show direction of polarization.

2011). The quasar possesses a peculiar radio structure on kiloparsec scales, with two diffuse lobes and a bent, knotty jet that appears to be disconnected from the lobes (see Fig. 1, *left*). On parsec scales (see Fig. 1, *right*) the quasar has a very compact core with an extended structure directed to the north. The jet is highly relativistic with an apparent speed up to 26.6 c (Lister *et al.* 2013). The object was detected at γ-rays during the EGRET era with a fairly flat spectral index for a quasar, 1.28±0.13 (Hartman *et al.* 1999). Since the *Fermi* Large Area Telescope (LAT) started operation in 2008 August, 1222+216 has exhibited three periods of high γ-ray activity. The first event, from early 2009 to early 2010 was the most dramatic. A second, milder event occurred at the end of 2012 and the third lasted from Spring 2013 into 2014 (see Fig. 2). During the first and the third events the source was detected at very high energies (VHE, E >100 GeV) by MAGIC (Aleksić *et al.* 2011) and VERITAS (Atel #5981), respectively. Further, during the most prominent event in 2010, the quasar varied at TeV energies on very short timescales, ∼10 min, while a single power law could fit the spectral energy distribution (SED) from several GeV to 400 GeV. The absence of a spectral cutoff constrains the γ-ray emission region to lie outside the BLR to avoid pair-production absorption of the VHE γ-rays.

We have been monitoring 4C+21.35 monthly with the Very Long Baseline Array (VLBA) at 43 GHz since 2007 June. We also observe the flux of the quasar at optical B, V, R, and I bands along with optical polarization measurements using different telescopes (see Jorstad *et al.* 2013 for details). Gamma-ray light curves of the quasar are constructed for 1 and 7 day integration intervals using *P7* photon and spacecraft data provided by the *Fermi* Science Support Center. Finally, we reduce and include X-ray and UV/optical data collected by the *Swift* XRT and UVOT. The multi-frequency data are presented in Figure 2. Here we discuss the inner jet behavior of the quasar during the dramatic high energy events. According to the current cosmological parameters, the luminosity distance of 4C+21.35 is 2.4 Gpc, for which the linear scale is 5.6 pc mas^{-1}. We use Reduced Julian Dates defined as RJD=JD-2450000.0.

https://doi.org/10.1017/S1743921315001829 Published online by Cambridge University Press

Table 1. Parameters of Superluminal Knots

Knot	N	μ mas yr^{-1}	β_{app} c	a mas	τ_{var} days	δ	Γ	$\Theta_\circ$ deg	$T_\circ$ RJD	T_1 RJD
B1	19	0.44±0.03	10.7±0.7	0.10±0.04	58±10	57	30	0.4	5313±29	5500±35
B2	22	0.49±0.02	11.9±0.4	0.09±0.04	142±19	19	13	2.7	5544±27	5754±39
B3	11	0.77±0.04	20.4±1.0	0.11±0.04	120±23	30	22	1.8	6241±33	6317±28
B4	3	0.87±0.16	21.3±4.0	0.10±0.03					6618±77	6685±36

Notes: N - number of epochs of knot observations, μ - proper motion; β_{app} - average apparent speed of the knot; a - angular size of the knot; τ_{var} - timescale of flux variability of the knot as defined by Burbidge *et al.* (1974); δ - Doppler factor; Γ - bulk Lorentz factor; $\Theta_\circ$ - viewing angle; $T_\circ$ - epoch of the passage of knot through the core, $A0$; T_1 - epoch of the passage of knot through feature $A1$.

2. Jet kinematics

Over the period from 2007 June to 2014 May we collected total and polarized intensity images of 1222+216 (along with other blazars) at 63 epochs The images can be found at website: **http://www.bu.edu/blazars/VLBA_GLAST/1222.html**. The data reduction is described in Jorstad *et al.* (2013). The final total and polarized intensity images (in Stokes parameters I, Q, and U) were modeled by circular components with Gaussian brightness distributions. Parameters of each component (flux, distance from the core, position angle with respect to the core, size of the knot, degree of polarization, and position angle of polarization) were compared across epochs to identify features with similar properties, either moving or stationary. As a result, we have found two approximately stationary knots: the core $A0$ and feature $A1$, plus 4 knots with superluminal apparent speeds, $B1$–$B4$. Figure 2 presents the light curve of the core, which shows variations by a factor of ∼10. Figure 3(a) shows the light curves of the moving knots, revealing fast decays, especially for knot $B1$. Figure 3(b) plots separation of the knots from the core as a function of time. Knots $B1$ and $B2$ executed non-ballistic motion, with acceleration after passing $A1$ 0.16±0.03 mas from the core. Table 1 gives the parameters of the moving knots. It also lists the Lorentz and Doppler factors and viewing angles of the knots, derived from the timescale of the flux decline of each knot, its VLBI size, and apparent speed (see Jorstad *et al.* 2005). Knot $B1$ has extreme relativistic parameters, with δ ∼60 and viewing angle $< 1°$. Table 1 also indicates epochs when each knot passed through the core, $T_\circ$, and stationary feature $A1$, T_1, while Figure 3(b) displays the correspondence between $T_\circ$ and T_1 and the timing of the peaks in the γ-ray flux. Figure 3(b) reveals excellent agreement between the periods of high γ-ray activity and epochs of passage of superluminal knots through the stationary features. All three active γ-ray states plus weak activity in the end of 2012 appear to be associated with propagation of superluminal disturbances in the inner jet. Note also that the duration of each active γ-ray state is at least ∼100 days. The sizes of the core and $A1$ are 0.03±0.02 mas and 0.07±0.02 mas, respectively, and the size of a superluminal knot is ∼0.1 mas (Table 1). If we assume that the speed of a knot in the core and $A1$ is the same as that of $B1$ and $B2$, it should take ∼100−130 days for a knot to pass through each stationary feature. This agrees very well with the duration of the γ-ray active states. In this case, stationary features should represent physical structures, e.g., recollimation shocks, while superluminal knots can be associated with moving shocks.

The radio light curve at 37 GHz (Fig. 2) shows an increase of brightness contemporaneously with the γ-ray activity, although the radio emission continues to be in an excited state from the beginning of 2009 through early 2014. We separate the light curves into two parts (2007−2011 and 2012−2014) to perform a correlation analysis. During the first part the radio light curve shows statistically significant correlation with the γ ray light curve with a delay of ∼265 days, while in the second part variations at the two

https://doi.org/10.1017/S1743921315001829 Published online by Cambridge University Press

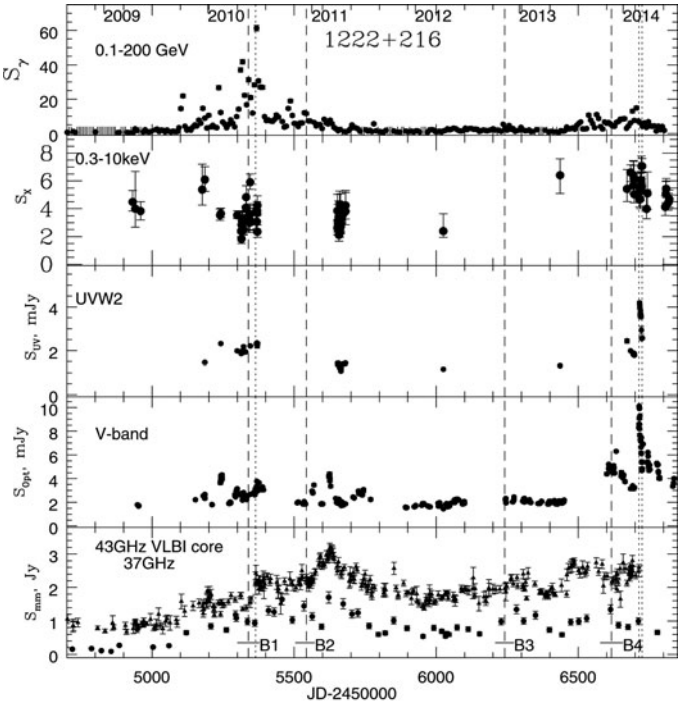

Figure 2. Light curves of 1222+216 at different frequencies; dashed lines show the ejection time of superluminal knots; dotted lines mark periods of detections at TeV energies.

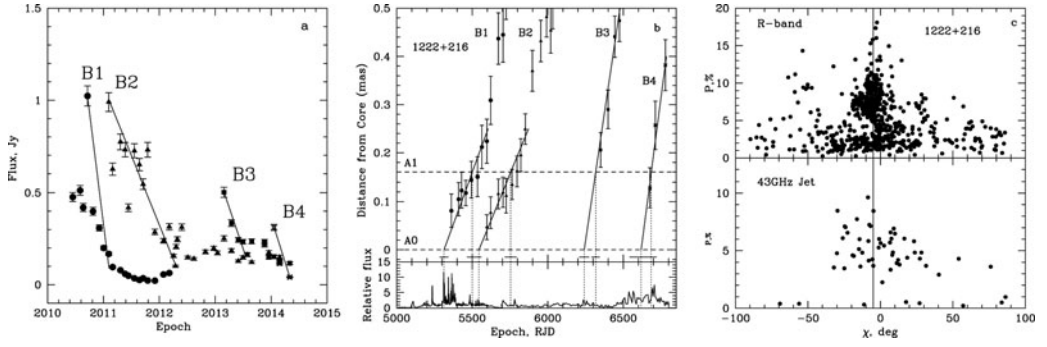

Figure 3. *a*: Light curves of moving knots $B1$ (circles), $B2$ (triangles), $B3$ (squares), and $B4$ (crosses); solid lines show slopes of the flux decay for each knot; *b (top):* Distance from the core vs. time for each knot. Solid lines show the best linear fit of the motion between $A0$ and $A1$, dashed lines mark the position of $A0$ and $A1$. The dotted lines show time of the passage of the knot through $A0$ and $A1$, while uncertainties of the times are shown by the horizontal solid segments. *b (bottom):* Relative γ-ray light curve constructed in two parts: RJD=5000−5700, normalized to 10^{-6} ph cm^{-2}s^{-1}, and RJD=5700−6850, normalized to 2×10^{-7} ph cm^{-2}s^{-1}. The dotted lines are the same as above. *c (top):* Dependence between degree and position angle of polarization at optical wavelengths; *c (bottom):* Dependence between p and χ of the jet integrated over the entire image at 43 GHz; solid line indicates the average direction of the jet.

wavelengths are simultaneous within ±5 days. Knots $B1$ and $B2$, ejected during the first outburst, were brighter than the core when they were separating from the core, and the difference between $T_\circ$ values of $B1$ and $B2$ are similar to the delay (see Table 1). Therefore, the delay between the γ-ray and radio light curves during the first outburst can be

https://doi.org/10.1017/S1743921315001829 Published online by Cambridge University Press

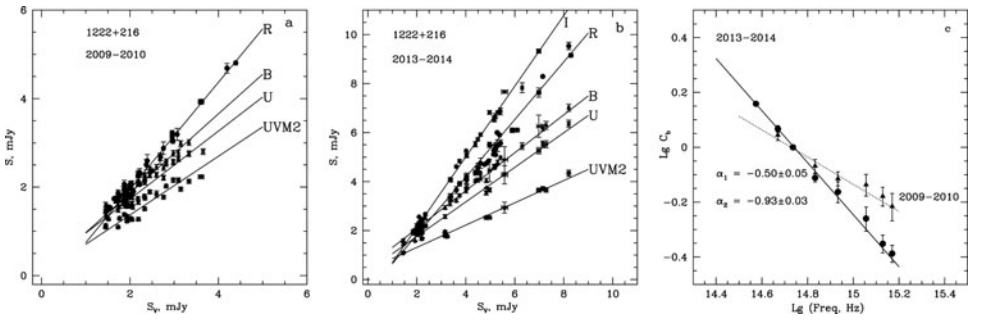

Figure 4. *a:* Flux in UVM2 (asterisks), U (crosses), B (triangles), and R (circles) bands vs. flux in V band during the first γ-ray event; *b:* Flux in UVM2 (asterisks), U (crosses), B (triangles), R (circles), and I (squares) bands vs. flux in V band during the last γ-ray event. Solid lines represent linear fits to flux-flux dependences. The data are corrected for Galactic extinction as described in Williamson *et al.* (2014); *c:* Relative SEDs of the non-thermal component during the first outburst (triangles, dotted line) and during the last outburst (circles, solid line)

explained by an increase in the opacity of the core, since during this period of 265 days either $B1$ or $B2$ was within the core.

3. Optical behavior

Figure 2 reveals an increase of optical emission during the first and last γ-ray events, and that the TeV detections coincide with optical flares. However, there is no statistically significant correlation between the γ-ray and optical light curves. Although the most prominent γ-ray event is observed in 2010, the most dramatic optical outburst occurred during the last γ-ray event when the amplitude of γ-ray and optical outbursts were quite similar. We have constructed the SEDs for the non-thermal emission during the first and last γ-ray events, which are remarkable for a quasar. Figure 4 presents flux-flux dependences for simultaneous measurements at different UV/optical wavelengths for the first (a) and second (b) periods. The dependences can be represented by linear fits; the logarithm of the slopes of the lines vs. the logarithm of the corresponding frequency gives a relative SED of the synchrotron component of the emission, since non-thermal emission is most likely responsible for the observed variability (Fig. 4c). The SEDs have very flat spectra: the value of $\alpha \sim -0.5$ ($S_\nu \propto \nu^\alpha$) during the first outburst is similar to that of HBLs, and $\alpha \sim -1.0$ during 2013-2014 is similar to α_{opt} of LBLs. This is a strong argument in favor of the enhanced synchrotron emission originating outside the BLR. In addition, the emission line flux does not show a connection with the continuuum (Smith *et al.* 2011).

Figure 3(c) shows the dependence of the degree of polarization on its position angle at optical wavelengths and in the jet at 43 GHz. Despite a higher degree of optical polarization in general, the distributions are quite similar with the highest values of p observed at position angles close to the jet direction. This implies that the magnetic field in the optical synchrotron emission region is similar to that in the jet and perpendicular to the jet direction when the degree of polarization is high, as expected for transverse and even oblique moving shocks.

4. Discussion

Our monitoring of the parsec-scale jet of the quasar 4C+21.35 reveals a close connection between the disturbances propagating in the jet and high γ-ray activity. Especially

https://doi.org/10.1017/S1743921315001829 Published online by Cambridge University Press

interesting is the case of the high energy outburst in 2009-2010 when short timescale variations at VHE were detected along with a superluminal disturbance in the jet with an extremely high Doppler factor. The very flat spectral index of the optical synchrotron continuum during this period was also observed to be uncharacteristically flat. Tavecchio *et al.* (2011) have proposed several models to fit the SED of the quasar from radio to TeV energies during this event, with the emission produced either by a very compact blob outside the BLR alone or paired with the emission of the more diffuse jet within or outside the BLR. Although the parameters of the models are not unique, the parameters of the blob are very similar to those that we have obtained from the VLBA monitoring, and the distribution of relativistic electrons is similar to that derived for the optical synchrotron component. Also, the Doppler factor of the underlying jet is quite high, $\sim$20. Our observations of the quasar with *Chandra* at 0.5-6 keV have detected X-ray emission on kiloparsec scales (Figure 1, *left*) that can be explained within the IC-CMB model if the jet is still relativistic on kiloparsec scales, with Doppler factor $\geqslant 17$ (Jorstad & Marscher 2006).

Another model to explain the observed multifrequency behavior of 4C+21.35 involves recollimation shocks (the core and quasi-stationary feature $A1$), through which the time-variable jet plasma flows (Marscher 2014). This model is supported by the good agreement between epochs of passage of moving knots through stationary features in the jet and peaks in the γ-ray light curve. Furthermore, we observe an increase in the degree of optical polarization along with an increase in the radio flux, as well as alignment of the position angle of polarization with the jet direction when the degree of polarization rises, as expected according to the model.

Acknowledgements

The research at Boston University was funded in part by NASA Fermi Guest Investigator grants NNX11AQ03G and NNX13AO99G, and Swift Fermi Guest Investigator grant NNX14AI98G. The VLBA data were obtained within the program VLBA-BU-BLAZAR. The VLBA is an instrument of the National Radio Astronomy Observatory which is a facility of the National Science Foundation operated under cooperative agreement by Associated Universities, Inc. The St. Petersburg group was supported in part by Russian RFBR grant 12-02-00452 and St.Petersburg University research grants 6.0.163.2010 and 6.38.71.2012. Optical monitoring of γ-ray-bright blazars at Steward Observatory is supported by NASA Fermi GI grants NNX08AW56G, NNX09AU10G, and NNX12AO93G. The Metsähovi team acknowledges the support from the Academy of Finland.

References

Aleksić, J., *et al.* 2011, *ApJL*, 730, L8
Burbidge, G. R., Jones, T. W., & O'Dell, S. L. 1974, *ApJ*, 193, 43
Farina, E.P., Decarli, R., Falomo, R., Treves, A., Raiteri, C. M. 2012, *MNRAS*, 424, 393
Hartman, R. C., *et al.* 1999, *ApJS*, 123, 79
Jorstad, S. G., *et al.* 2013, *ApJ*, 773, 147
Jorstad, S. G. & Marscher, A. P. 2006, *Astronomische Nachrichten*, 327, 227
Jorstad, S. G., *et al.* 2005, *AJ*, 130, 1418
Lister, M. L., *et al.* 2013, *AJ*, 146, 120
Malmrose, M. P., Marscher, A. P., Jorstad, S. G., Nikutta, R., & Elitzur, M 2011, *ApJ*, 732, 116
Marscher, A. P. 2014, *ApJ*, 780, 87
Smith, P. S., Schmidt, G. D., & Jannuzi, B. T. 2011, *2011 Fermi Symposium proceedings - eConf C110509*, arXiv:1110.6040
Tavecchio, F., *et al.* 2011, *A&A*, 534, 86
Williamson, K. E., *et al.* 2014, *ApJ*, 789, 135